Published in final edited form as:

Nature. 2011 February 24; 470(7335): 543–547. doi:10.1038/nature09737.

Programming the magnitude and persistence of antibody responses with innate immunity

Sudhir Pai Kasturi[1,2], **Ioanna Skountzou**[1,3], **Randy A. Albrecht**[4], **Dimitrios Koutsonanos**[3], **Tang Hua**[1,2], **Helder Nakaya**[1,2], **Rajesh Ravindran**[1,2], **Shelley Stewart**[5], **Munir Alam**[5], **Marcin Kwissa**[1,2], **Francois Villinger**[1,2,6], **Niren Murthy**[7], **John Steel**[4], **Joshy Jacob**[1,2,3], **Robert J. Hogan**[8], **Adolfo García-Sastre**[4,9,10], **Richard Compans**[1,3], and **Bali Pulendran**[1,2,6,*]

[1]Emory Vaccine Center, Emory University, Atlanta GA 30329

[2]Yerkes National Primate Research Center, Emory University, Atlanta GA 30329

[3]Department of Microbiology and Immunology, Emory University, Atlanta, GA

[4]Department of Microbiology, Mount Sinai School of Medicine, New York, NY

[5]Duke Human Vaccine Institute, Duke University Medical Center, Durham, NC

[6]Department of Pathology, Emory University School of Medicine, Atlanta, GA

[7]The Wallace H. Coulter Department of Biomedical Engineering, Georgia Institute of Technology, Atlanta

[8]Department of Anatomy and Radiology, College of Veterinary Medicine, University of Georgia, Athens, GA

[9]Department of Medicine, Division of Infectious Diseases, Mount Sinai School of Medicine, New York, NY

[10]Global Health and Emerging Pathogens Institute, Mount Sinai School of Medicine, New York, NY

Abstract

Many successful vaccines induce persistent antibody responses that can last a lifetime. The mechanisms by which they do so remain unclear, but emerging evidence suggests that they

Corresponding Author, Bali Pulendran, Ph.D., Emory Vaccine Center, 954 Gatewood Road, Atlanta, GA 30329, USA, Tel: 404 727 8945, Fax: 404 727 8199, bpulend@emory.edu.

Supplementary Information is linked to the online version of the paper at www.nature.com/nature.

Author Contributions: S.P.K and B.P designed the study, planned the experiments, analyzed the data. B.P wrote the manuscript. S.P.K, I.S and B.P designed and performed the H1N1 vaccine studies in mice and primates. D.K assisted with the H1N1 vaccine studies in mice and primates. R.A.A, A.G.S and J.S designed and performed the neutralization assays and challenge experiments with H5N1 vaccine studies in mice. T.H and R.R assisted with experiments. H.N performed the microarray analysis. S.S and M.A designed and carried out the SPR based avidity experiments. M.K assisted with design and execution of mice and NHP experiments. N.M assisted with design of formulations. JJ assisted with immunohistochemistry and design of experiments. RJH expressed and purified the recombinant H5HA protein. RWC helped plan and design H1N1 vaccine study in mice and primates.

Author Information: The authors declare no competing financial interests. All microarray data are deposited in Gene Expression Omnibus under accession number GSE25677.

activate dendritic cells (DCs) via Toll-like receptors (TLRs)1,2. For example, the yellow fever vaccine YF-17D, one of the most successful empiric vaccines ever developed3, activates DCs via multiple TLRs to stimulate pro-inflammatory cytokines4,5. Triggering specific combinations of TLRs in DCs can induce synergistic production of cytokines6, which results in enhanced T cell responses, but its impact on antibody responses remain unknown. Learning the critical parameters of innate immunity that programs such antibody responses remains a major challenge in vaccinology. Here we demonstrate that immunization of mice with synthetic nanoparticles containing antigens plus Toll-like receptor (TLR) ligands 4 + 7 induces synergistic increases in antigen-specific, neutralizing antibodies compared to immunization with a single TLR ligand. Consistent with this there was enhanced persistence of germinal centers (GCs), and of plasma cell responses, which persisted in the lymph nodes for >1.5 years. Surprisingly, there was no enhancement of the early short-lived plasma cell response, relative to that observed with single TLR ligands. Molecular profiling of activated B cells, isolated 7 days after immunization, indicated early programming towards B cell memory. Antibody responses were dependent on direct triggering of both TLRs on B cells and dendritic cells (DCs), as well as on T-cell help. Immunization protected completely against lethal avian and swine influenza virus strains in mice, and induced robust immunity against pandemic H1N1 influenza in rhesus macaques.

We designed a nanoparticle based vaccine, similar to a virus in size and composition. A biodegradable synthetic polymer poly(D,L-lactic-co-glycolic acid), (PLGA)7, was used to synthesize ~300nM sized nanoparticles containing the TLR ligands MPL (TLR4), R837 (TLR7), or both ligands, together with an antigen (Supplementary Fig. 1). Immunization of mice with nanoparticles containing MPL+R837 (PLGA(MPL+R837)) plus antigen induced enhanced antibody and T cell responses, compared to immunization with soluble antigen plus MPL+R837 (data not shown). Consistent with recent observations8,9, delivery of antigen and TLR ligands in separate nanoparticles induced a stronger antibody response, than delivery of both in the same nanoparticle (Supplementary Fig. 2). Initially, cohorts of C57BL/6 mice were immunized with nanoparticles containing chicken ovalbumin (OVA) (PLGA(OVA)) alone, or together with PLGA(MPL), PLGA(R837), or (PLGA(MPL+R837). OVA emulsified in alum, was used as a control. Immunization with PLGA(MPL) or PLGA(R837) plus nanoparticles containing 50μg or 10μg (Supplementary Fig 3a&4a), induced enhanced OVA-specific antibody titers after immunization. Strikingly, there was a synergistic enhancement of the antibody titers in mice that received PLGA(MPL+R837) (Supplementary Figs 3a&4a). Secondary immunization with the same immunogen 5 weeks later markedly increased titers in all groups, with the synergy effect with PLGA(MPL +R837) still evident, especially at the lower 10μg dose (Supplementary Figs. 3b&4b). Thus in all following experiments we used 10μg of antigen. In addition to OVA, we also used other antigens including the protective antigen (PA) from *Bacillus anthracis*10 (Supplementary Fig. 5), and hemagglutinin (HA) from avian influenza H5N1 virus11(Fig. 1). As observed with OVA, there was a synergistic enhancement in the antigen-specific antibody responses after primary and secondary immunization of mice with PLGA(MPL +R837) plus PLGA(PA) (Supplementary Fig. 5 a, b), or PLGA(HA) (Fig. 1a, b).

The avidity of antigen-antibody binding is one index of the quality of the antibody response12. We used a surface plasmon resonance (SPR) assay to assess avidity. Sera from

animals immunized with PLGA(MPL+R837) plus PLGA(HA) gave the highest binding response (Fig. 1c). The slower dissociation and higher association rates indicate that immunization with PLGA(MPL+R837) plus PLGA(HA) induced enhanced high affinity antibody response than that induced by PLGA(MPL) or PLGA(R837) plus PLGA(HA). A similar trend was also observed with PA as an antigen (Supplementary Fig. 5c). Consistent with the effects on ELISA titers and avidity, mice immunized with PLGA(MPL+R837) plus PLGA(HA) had the greatest neutralization antibody titers (Fig. 1d).

We next assessed the mechanism by which PLGA(MPL+R837) induced synergistic responses. PLGA(MPL+R837) enhanced the secretion of the pro-inflammatory cytokines by DCs *in vitro*, compared to PLGA(MPL) or PLGA(R837) (Supplementary Fig. 6a). Furthermore, *in vivo* depletion of DCs in the CD11c-DTR mice13, or Langerhans cells using the Langerin-DTR mice14, resulted in diminished antibody titers (Supplementary Fig. 6b,c). These data demonstrate a critical role for DCs in mediating the antibody response to immunization with PLGA(MPL+R837). Signaling via TLR 4 and 7 is dependent on the adaptor proteins MyD88 or TRIF; MPL is reported to signal predominantly via TRIF15. Both MyD88 and TRIF were required for antibody responses stimulated by PLGA(MPL +R837) plus PLGA(OVA) (Supplementary Fig. 7).

B cells express and respond to TLRs16,17. Thus, we determined whether direct triggering of TLRs on B cells was essential for antibody responses. *In vitro* stimulation naïve splenic B cells with PLGA(MPL+R837) synergistically enhanced B cell proliferation, relative to stimulation with PLGA(MPL) or PLGA(R837) (data not shown). To assess this effect *in vivo*, mice lacking B cells (μMT mice) were reconstituted with B cells from wild type (WT) mice, or *MyD88*$^{-/-}$ or *TRIF*$^{-/-}$ mice, and then immunized with PLGA(MPL+R837) plus PLGA(OVA) (Fig. 2a). In μMT mice reconstituted with "WT B cells," immunization induced a synergistic enhancement of antibody responses (Fig. 2b). However, μMT mice reconstituted with *MyD88*$^{-/-}$ or *TRIF*$^{-/-}$ B cells had diminished antibody titers (Fig. 2c), demonstrating that direct TLR triggering on B cells was required for stimulation of antibody responses. We then determined whether the synergy was dependent on co-expression of TLR4 and TLR7 on the same B cell, or whether there could be complementation between B cells lacking different TLRs. We thus transferred B cells from *TLR4*$^{-/-}$ mice, or *TLR7*$^{-/-}$ mice, or a 1:1 mixture of B cells from *TLR4*$^{-/-}$ and *TLR7*$^{-/-}$ mice into μMT mice. Immunization with PLGA(MPL+R837) and PLGA(OVA) demonstrated a requirement for co-expression of both TLRs on the same B cell (Fig. 2d).

Finally, TLR activation of DCs is known to stimulate antigen-specific CD4+ T helper cells, which are essential for induction of antibody responses 18. Depletion of CD4+ T helper cells prior to immunization diminished antibody responses (Supplementary Fig. 8). Consistent with this, immunization with PLGA(MPL+R837) and PLGA(OVA) resulted in enhanced antigen-specific CD4+ T cell response (Fig. 2e). Interestingly, we observed (Fig. 2f), that OVA-specific CD4+ T helper responses was substantially reduced in μMT mice transferred with *MyD88*$^{-/-}$ or *TRIF*$^{-/-}$ B cells, (in which the antibody responses were severely compromised, (Fig. 2c)), suggesting a requirement for activated B cells in mediating enhanced activation of CD4+ T-helper cells, as demonstrated previously19.

Antibody responses develop along two anatomically and functionally distinct pathways20. The extrafollicular pathway rapidly generates short lived, antibody producing cells (plasma cells), and the GC pathway generates memory B cells and long lived plasma cells that secrete high affinity antibody20. We determined whether immunization with nanoparticles containing different adjuvants differentially regulated the two pathways. Thus, mice immunized with the different adjuvants were sacrificed at day 7, lymph nodes isolated and the presence of antibody producing plasma cells evaluated by immunohistology. There was no apparent difference in the IgG+ plasma cells, at day 7, between mice immunized with various adjuvants (Supplementary Fig. 9). We also investigated the kinetics of GC formation following immunization. Strikingly, mice immunized with both TLR ligands had a greatly enhanced and sustained GC response compared to those immunized with a single TLR ligand, (Supplementary Fig. 9, Fig. 3a,b). At day 28 there were approximately 10–12 per GCs per lymph node and at day 42 there were about 6 GCs per lymph node, significantly higher than the numbers observed in lymph nodes of mice immunized with single TLR ligands (Fig. 3a & b). By 8 weeks post immunization the numbers of GCs was still substantially higher in the PLGA(MPL+R837) group than in the other groups (Fig. 3b). This demonstrates that PLGA(MPL+R837) preferentially enhances the GC pathway.

Furthermore, assessment of antigen-specific IgG secreting plasma cells by the ELISPOT assay, indicated no differences in the numbers of plasma cells at day 7 in the MPL alone versus MPL+R837 groups (Fig. 3c). At day 28 there were enhanced numbers of plasma cells in the PLGA(MPL+R837) group, relative to single TLR ligand groups. Secondary immunization with the same antigen + adjuvant, resulted in a profoundly enhanced and sustained memory response in the PLGA(MPL+R847) group (Fig. 3c). Strikingly, there was a persistent plasma cell response in the lymph node for >1.5 years. Interestingly, there was no corresponding enhancement in the numbers of antigen-specific plasma cells in the bone marrow, (a known destination for plasma cell21), in the PLGA(MPL+R837) group, relative to the single TLR ligand groups (data not shown). This demonstrates that immunization with PLGA(MPL+R837) preferentially enhances memory B cell generation. Consistent with this, FACS analysis22 revealed enhanced numbers of isotype switched, antigen-specific B cells in the PLGA(MPL+R837) group relative to the PLGA(MPL) or PLGA(R837) groups, during the memory phase after a secondary boost, but no such enhancement early during the primary response (Supplementary Fig. 10).

The effects of PLGA(MPL+R837) o n the GC pathway might have occurred via early programming of antigen-specific B cells, or as a result of the continued presence of antigen and/or adjuvant. To determine whether there was any early programming of B cells, we isolated isotype switched, antigen-experienced B cells by FACS at 7 days post immunization with nanoparticles containing various adjuvants plus OVA, and performed microarray analyses to assess their molecular signatures. Strikingly, there was a great enrichment for genes expressed in memory B cells23, in the cells isolated from mice immunized with PLGA(MPL+R837) and PLGA(OVA), relative to mice immunized with a single TLR ligand (Supplementary Fig. 11a–c). Such genes included *Bcl-2, Bcl11a, Tank*, several type I IFN related genes, *Plcg2 and CD38*, which are known to play key roles in memory B cell formation and, several genes that regulate the survival, proliferation and differentiation of

GC B cells, such as, *IL-17ra, IL-18r1, Pax5, Ifngr2-, Bcor, Ikzf1* (Supplementary Fig. 11a,b). These data suggest that immunization with antigen and MPL+R837 stimulates early programming to the GC/memory pathway.

We next determined whether immunization also enhanced antigen-specific memory T cell responses. There was a synergistic enhancement of OVA-specific IFNγ-producing CD4+ T helper cell responses at 8 weeks post secondary immunization (Supplementary Fig. 12a,b), but not at days 7 or 14 post primary immunization (data not shown), indicating a preferential effect on the generation of memory T cells. Similar results were observed in mice immunized with HA and PA antigen, even 1.5 years post immunization (Supplementary Fig. 12c–f). PLGA(MPL+R837) immunization also enhanced the antigen specific CD8+ T cell responses. Although no synergistic enhancement was observed in the frequencies of IFN-γ producing, OVA-specific CD8+ T cells at day 7 post primary immunization, there was an increase at day 7 post secondary immunization (Supplementary Fig. 13). Polyfunctional T cells secreting multiple cytokines such as IFN-γ, TNF-α and IL-2 have been implicated in mediating enhanced protection24. We also observed enhanced numbers of triple (IFN-γ, TNF-α and IL-2) and double cytokine (IFN-γ, IL-2) producing CD8+ T cells in mice immunized with PLGA(MPL+R837) (Supplementary Fig. 14a,b). Thus, PLGA(MPL+R837) enhances the magnitude and quality of the antigen specific memory CD4+ and CD8+ T cells. To assess the relevance of enhanced B and T cell responses for protective immunity, we evaluated efficacy of these vaccines in mediating protection in mice, against the 2009 pandemic H1N1 influenza A virus11(Supplementary Fig. 15,16), and the H5N1 avian influenza virus 11,25 (Supplementary Fig. 17). In each case, there was enhanced antigen-specific humoral immunity and survival against lethal infection of mice (Supplementary Fig. 15–17).

Finally we assessed the immunogenicity of PLGA(MPL+R837) in non human primates. In humans and non human primates, unlike in mice, TLR7 is selectively expressed on plasmacytoid DCs, and not on myeloid DCs 2. Since multiple DC subsets appear to be involved in the stimulation of antibody responses by PLGA(MPL+R837) (Supplementary Fig 6b,c), we used R848, that signals through both TLR7 and TLR8 2,26. Furthermore, in humans although naïve B cells do not express TLRs 4, 7 or 8, activated B cells including plasma cells upregulate and respond to these TLRs 27. Current human monovalent vaccines against H1N1 influenza contain 15μg of HA (effectively 45μg of whole inactivated virus)28. We therefore used 50μg of WIV (~16μg HA), as well as a 5-fold lower dose (~3μg HA), with and without adjuvant, to determine whether there was a dose sparing effect. 4 cohorts of 4 rhesus macaques per cohort were immunized subcutaneously with the indicated doses of WIV, with or without PLGA(MPL+R837) or PLGA(MPL+R848) (Fig. 4a). After a single immunization with 10μg or 50μg of WIV without any adjuvants, there was no detectable antibody response (Fig. 4b–d). In contrast, adjuvanting with PLGA(MPL+R848) induced robust antibody responses, as early as 2 weeks (Fig. 4b–d). Immunization with PLGA(MPL +R837) yielded enhanced binding antibodies, but had more modest effects on HAI and neutralization titers (Fig. 4b–d). Notably, the magnitude of HAI and neutralization titers 28 days after a single immunization with PLGA(MPL+R848) much greater than 1/40, considered the correlate of protection against influenza in humans. (Fig. 5c&d)29. There

was at least a 5-fold “dose sparing” effect, since 10μg of antigen plus PLGA(MPL+R848) yielded a much greater response than that induced by 50μg of antigen alone (Fig. 5b–d). Secondary immunizations, enhanced the antibody responses in all of the groups, and although PLGA(MPL+R848) still induced the strongest response, PLGA(MPL+R837) also induced responses greater than that required for protection (Fig. 5c&d). Furthermore, the dose sparing effect was still evident, after secondary immunization (Fig. 5b–d).

Here we have described a nanoparticle based vaccine that resembles a virus in size and composition, and that recapitulates the immunogenicity of live viral vaccines5. A striking feature of the immune response stimulated by this vaccine is in the induction of long lived GCs and persistent antigen-specific B and T cell responses, similar to that seen with viral infections30. Importantly, although all TLR ligands stimulate primary antibody responses, the combined TLR4+TLR7 stimulus enhances the GC pathway of memory B cell formation and long lived plasma cell responses, far more efficiently than stimulation with single TLR ligands (Supplementary Fig 18). The molecular signatures of antigen-activated B cells isolated early after immunization, suggests early programming towards a quasi memory state (Supplementary Fig 11), but it is also likely that persistent antigen/adjuvants, as evidenced by persistent immune complexes in GCs (Fig. 3) play a role. A curious aspect of our data is the requirement for the TLR ligands and antigens to be delivered on 2 separate particles, consistent with other studies8,9. From a practical perspective, this offers flexibility in coupling a generic adjuvant containing particle, with another particle containing antigen from any pathogen. Furthermore, as each of the components of this vaccine (MPL, R837, PLGA) have been licensed for human use, this vaccine formulation may provide a universal platform for vaccine design against pandemics and emerging infections.

Methods Summary

Synthesis and characterization of nanoparticles

Antigens were encapsulated in PLGA nanoparticles using a water in oil in water (w/o/w) emulsion technique. MPL was encapsulated in PLGA formulations using an oil in water (o/w) single emulsion process as described before with slight modifications8. Sizing of the nanoparticles was conducted using a dynamic light scattering, and protein loading assessed described before31.

Immunization of mice and non human primates

8–12 week old BALB/c or C57BL/6 mice (Charles River) were immunized with 10μg of antigen encapsulated in nanoparticles suspended in 200μl of PBS subcutaneously at the base of the tail. 10–13 year old female Rhesus Macaques (7–10kg) were used were immunized subcutaneously in the right leg. All procedures were performed in accordance Emory School of Medicine IACUC guidelines.

BIACORE antigen antibody affinity binding analysis

SPR binding measurements were carried out on a BIAcore™ 3000 instrument (BIAcore/GE Healthcare).

H5N1 Microneutralization assays was performed as described earlier25.

B cell ELISPOT

1×10^6 lymph node cells were serially diluted and cultured overnight in duplicate wells of ovalbumin coated nitrocellulose lined 96 well plates (Millipore). Cells were discarded and wells were treated with biotinylated goat anti mouse total IgG (Southern Biotech) in PBS/ 0.5% Tween 20 +1% FBS for 1.5 hours at room temperature. Wells were washed and treated with Streptavidin Alkaline phosphatase (Vector Labs) for another 1.5 hours at room temperature. Finally, NBT/BCIP colorimetric substrate for alkaline phosphatase was added to the wells and the reaction was stopped after visualization of purple colored spots.

Affymetrix Gene Chip Analysis

Total RNA from sorted B-cells was purified using Trizol® (Invitrogen). All RNA samples were checked for purity and for integrity, and amplified, processed through EXON Module, fragmented and labeled. Labeled targets hybridized to GeneChip® Mouse Gene 1.0ST arrays (Affymetrix).

Methods

Encapsulation of antigens and TLR ligands in nanoparticles

Antigens were encapsulated in poly (D,L-lactic-co-glycolic acid), PLGA nanoparticles using a water in oil in water (w/o/w) emulsion technique. Briefly, 200μl of protein solution (PBS + 0.5% polyvinyl alcohol (PVA) as an excipient (Sigma Aldrich, St Louis, MO)), ovalbumin grade VI (Sigma Aldrich, St Louis, MO) at 50mg/ml, *Bacillus anthracis* protective antigen (PA; List Laboratories, San Diego, CA) at 15mg/ml, and A/Vietnam/1203/2004 specific haemagglutinin protein (H5HA; affinity chromatography purified from 293 HEK cells) at 15mg/ml were homogenized with 10% wt/v PLGA (RG502H, Bohreinger Ingelheim, Germany) in dichloromethane (200mgs in 2ml) with the Powergen homogenizer (Fisher Scientific, PA) at speed 5, for 1.5 minutes. The water in oil emulsion (w/o) was then added to 15ml of 5% wt/v solution of PVA for the second emulsion step identical to the first emulsion process described above, at speed 5. The water in oil in water (w/o/w) double emulsion was then subjected to solvent evaporation for 4 hours at room temperature.

MPL was encapsulated in PLGA formulations using an oil in water (o/w) single emulsion process as described before with slight modifications8. MPL (detoxified lipid A, Avanti Lipids, Alabaster, AL) was dissolved in chloroform at 5mgs/ml and TLR7 ligand R837 (Invivogen, CA) was dissolved at 10–20mg/ml in DMSO with heating. R848 was dissolved at 12.5mg/ml in dichloromethane. MPL, 0.5ml at 5mg/ml was added to 200mgs of PLGA polymer dissolved in 2.0 ml of dichloromethane. For particles containing both MPL and R837, 0.5ml or 5mgs of R837 in DMSO was added to the mixture of PLGA and MPL. For particles containing both MPL and R848, 8mgs of R848 in dichloromethane was added to the mixture of PLGA and MPL. For particles used in non human primate studies, 0.1ml of 5mg/ml MPL, 0.5ml or 10mgs of R837 and 12.5mgs of R848 was added to 200mgs of PLGA polymer in 2.0ml of dichloromethane. The organic phase containing PLGA with MPL and/or R837 or R848 was homogenized with 15ml of a 5% wt/v PVA solution for 2

min using a speed setting 6 at room temperature. The oil in water emulsion (O/W) was then added to 85ml of a 5% wt/v solution of PVA surfactant to evaporate the organic solvent for 4 hours at room temperature. The nanoparticles formed were centrifuged at 3500×g for 20 minutes and washed with 50 ml of 0.2μm filter sterilized, deionized water 3 times. Nanoparticles were snap frozen in liquid nitrogen and lyophilized using a Freezone 2.5L benchtop lyophilizer (Labconco, MO, USA).

Nanoparticle Characterization

Sizing of the nanoparticles was conducted using a dynamic light scattering based sizer (90PLUS) from Brookhaven Instruments (Holtsville, NY). Sizes are represented as the mean diameter of the volume average size distribution ± standard deviation, of different batches. Protein encapsulation levels were estimated as described before, using a BCA assay (Pierce Biotechnology, Rockford, IL)31. UV-Vis scan using a Cary Win50 UV-Vis spectrophotometer yielded a peak absorbance for R837 at 325nm (327nm for R848) and encapsulation was estimated using a standard curve of R837 or R848 in DMSO and NaOH/SDS. MPL encapsulated in nanoparticles was used in splenic DC stimulation experiments with known concentrations of soluble MPL yielding identical cytokine production and estimated at 100% encapsulation efficiency.

Mouse DC culture

CD11c+ DCs were isolated from spleens of naïve C57BL/6 mice. Spleens were digested with collagenase type IV (Worthington Chemicals, NJ), and CD11+c cells were enriched by positive selection using anti mouse CD11c magnetic beads using manufacturer's instructions (Miltenyi Biotech, Auburn, CA). DCs (1×10^6 cells/ml) were cultured in 48 well culture plates with PLGA encapsulated TLR ligands for 24 hours.

Mice

IL-6$^{-/-}$ and *TICAM-1*$^{lps2/lps2}$ (Jackson labs, Bar Harbor, Maine). *IFNα/βR*$^{-/-}$ (Dr. Samuel Speck, Emory University, Atlanta). *MyD88*$^{-/-}$ and *TLR-7*$^{-/-}$ (Dr. Shizuo Akira, Osaka). *TLR4*$^{-/-}$ (Dr. Koichi Kobayashi, Dana Farber Cancer Institute, Boston, MA).

Immunization of mice and non human primates

8–12 week old BALB/c or C57BL/6 mice (Charles River Laboratories, Wilmington, MA) were immunized with 10μg of antigen in nanoparticles (suspended in 200μl of PBS), subcutaneously at the base of the tail. TLR ligands in were co-delivered with protein encapsulated nanoparticles. 3mgs of PLGA particles containing MPL, R837 or MPL+R837 containing 37.5μg of MPL and 60μg of R837 were used. Imject Alum (Pierce/ThermoScientific, Rockford, IL) was used to adsorb protein at a 1:1 volume ratio as per the manufacturer's instructions. Mice were bled via the lateral tail vein at regular intervals after primary and secondary immunizations and serum isolated for analysis of antibody responses by ELISA assays. CD11c+ DTR mice13 were immunized 24 hours post -DC depletion. Langerin-DTR mice14 were immunized 3 weeks post depletion, when there is replenishment of Langerin+ DCs in the dermis and lymph nodes, but not in the epidermis32. CD4+ T cells were depleted with an anti mouse CD4+ antibody (Clone GK1.5 kindly

provided by Dr. Robert Mittler, Emory) injected at 250μg/mouse as described33. 10–13 year old female Rhesus Macaques (7–10kg) were used. Animals were immunized subcutaneously in the right leg. All animal procedures were performed in accordance with guidelines established by the Emory School of Medicine IACUC.

Antibody ELISA

96 well Nunc maxisorp plates (Nunc, Denmark) were coated with 100μl of 20μg/ml of ovalbumin, 1μg/ml of PA or 0.5μg of H5HA protein overnight at 4° C. Plates were washed 3 times with PBS/0.5% Tween 20 using a Biotek auto plate washer and blocked with 200μl of 4% non fat dry milk (Biorad, Hercules, CA) for 2 hours at room temperature. Serum samples from immunized mice at the indicated time points were serially diluted in 0.1% non fat dry milk in PBS/0.5% Tween 20 and incubated on blocked plates for 2 hours at room temperature. Detection antibodies (Southern Biotech, Birmingham, AL). Wells were washed and incubated with anti mouse IgG2c-horse radish peroxidase(HRP) conjugate (1:2000), anti mouse IgG2b biotin conjugate(1:2000), anti mouse IgG1-HRP conjugate(1:5000) and streptavidin-HRP conjugate (1:5000) in PBS/0.5% Tween 20 for 2 hours at room temperature. Plates were washed and developed using 100μl per well of tetramethylbenzidine (TMB) substrate (BD Biosciences, San Diego, CA) and stopped using 2N H_2SO_4. Plates were analyzed using a BioRad plate reading spectrophotometer at 450nm with correction at 595nm. Antibody titers were represented as serum reciprocal dilution yielding ≥ 0.1 O.D value at 450nm. Antibody levels (ng/ml) in H1N1 whole inactivated virus (WIV) immunized mice were assayed as previously described 34. To analyze WIV specific antibody levels in rhesus macaques, the assay was performed as described for mice. A capture rhesus IgG (Clone:SB108A) was used to establish a standard curve with the rhesus IgG standards (Cat#0135-01; Southern Biotech). 2μg/ml of WIV was used to coat NUNC maxisorp plates overnight and plates were blocked with 4% non fat dry milk. Rhesus plasma samples were used at appropriate dilutions for prime and boost and incubated for 2 hours at room temperature. Plates were washed 5× with PBS/0.5%Tween-20 using an automated plate washer and a goat anti rhesus HRP was used at 1:4000 dilution for 1 hour at room temperature, washed and developed with TMB substrate. Antibody concentrations were calculated from the IgG standard curves and represented as μg/ml.

BIAcore assay

Surface plasmon resonance (SPR) binding measurements were carried out on a BIAcore™ 3000 instrument (BIAcore/GE Healthcare, Pittsburgh, PA), as described earlier35. Serum samples were injected at a 1:50 dilution in PBS for 5 minutes at a flow rate of 10 μL/min. Binding to the negative control rPA surface was subtracted from each sample curve and binding response was measured at 15 and 500 seconds after the end of the injection. As a measure of antigen specific antibody binding avidity, maximal response unit (Binding RU) and dissociation rates were measured. Maximal binding RU was measured after subtraction of non-specific signal on the control surface at 15 seconds post injection and normalized dissociation was calculated as a ratio of late to early binding responses over a dissociation phase of 500 seconds. Following each injection cycle, chip surfaces were regenerated with a short injection of 25 mM NaOH.

H5N1 Microneutralization assays

Serum samples from H5HA immunized mice were tested for their ability to neutralize a recombinant (6:2) A/PR/8/34 Influenza A virus expressing the A/Vietnam/1203/2004 H5HA and N1NA in cell culture in vitro as described earlier25.

Histology and Immunofluorescence

Draining inguinal lymph nodes were isolated and snap frozen in molds containing OCT medium, dropped into 2-methyl butane cooled with liquid nitrogen. Frozen lymph nodes were sectioned at 5μm, fixed in ice cold acetone for 10 minutes, air dried and stored at −80°celcius. Sections were fluorescently stained with Dylight488 labeled anti mouse total IgG (Jackson Immunoresearch, West Grove, PA), Alexa647 labeled anti mouse B220 or GL-7 (Ebioscience, San Diego, CA), followed by Alexa555 conjugated Streptavidin (Invitrogen, Carlsbad, CA). Fluorescent images were captured using a 5× and 20 × objectives on a Zeiss Axioscope (Carl Zeiss, Germany).

B cell ELISPOT

1×10^6 lymph node cells were serially diluted and cultured overnight in duplicate wells of ovalbumin coated nitrocellulose lined 96 well MAHA ELISPOT plates (Millipore, Bedford, MA). Cells were discarded and wells were treated with biotinylated goat anti mouse total IgG (Southern Biotech, Birmingham, AL) in assay buffer (PBS/0.5% Tween 20 +1% FBS) for 1.5 hours at room temperature. Wells were washed and treated with Streptavidin Alkaline phosphatase (Vector Labs) at 1:500 for 1.5 hours at room temperature. NBT/BCIP colorimetric substrate for alkaline phosphatase was added to the wells and the reaction was stopped after visualization of purple colored spots. # of ELISPOTS/well were counted using an ImmunoSpot ELISPOT reader and represented as # of ELISPOTS (Antibody secreting cells) per total 1×10^6 lymph node cells.

CD4+ T cell assays

1×10^6 lymph node cells were cultured in a 200μl volume with 100μg/ml of ovalbumin protein or 5μg/ml of PA or 5μg/ml of H5HA in 96 well round bottomed plates for 4 days. Cells were transferred to anti CD3 (10μg/ml) and anti CD28 (2μg/ml) coated flat bottomed 96 well plates for 6 hours in the presence of Golgi plug (1μg/ml) (BD Biosciences, San Diego, CA). Cells were stained for surface CD4 using Percp anti mouse CD4 (Clone; RM4–5) for 30 minutes at 4°C. Cells were washed 3× with FACS buffer, fixed and permeabilized using BD Cytofix/Cytoperm and stained for intracellular IFN-γ using APC conjugated anti mouse IFN-γ (Clone; XMG1.2) for 30 minutes in 1X BD perm/wash solution at 4°C. Cells were washed with perm wash followed by FACS buffer and acquired on a FACS Caliber cytometer. FACS data was analyzed using the Flow Jo software (Tree Star Inc, OR).

CD8+ T cell assays

Primary and memory CD8+ T cell responses were evaluated at day 7 post primary and secondary immunizations. Briefly, peripheral blood mononuclear cells (PBMCs) were enriched using a sucrose density gradient separation (Histopaque, Sigma Aldrich, MO) and cultured with ovalbumin specific MHC class I restricted peptide at 1μg/ml (SIINFEKL) for

restimulation ex-vivo in the presence of brefeldin A (5μg/ml). Stimulated cells were stained for intracellular cytokines using established protocols from BD Biosciences as explained for CD4+ T cell staining experiments above. Cells were stained with Percp conjugated anti mouse CD8α (Ly-2) (Clone; 53-6.7), APC conjugated anti mouse IFN-γ (Clone; XMG1.2), FITC conjugated anti mouse TNF-α (Clone; MP6-XT22) and PE conjugated anti mouse IL-2 (Clone; JES6-5H4). Labeled cells were acquired on a FACS Caliber cytometer and FACS data was analyzed using Flow JO software (TreeStar Inc., OR).

B cell multi color flow cytometry

Antibodies used: PE labeled anti mouse IgG (Jackson Immunoresearch, West Grove, PA), Percp labeled anti mouse CD19 (Clone; 6D5, Biolegend, San Diego, CA), E-fluor 405 labeled anti mouse IgD (Ebioscience), Alexa430 succinimidyl ester for live/dead cell discrimination (Invitrogen), biotin conjugated anti mouse Ly77/GL7 (Clone; GL-7, Ebioscience), APC labeled anti mouse CD138 (clone;281-2, BD Biosciences), APC-Cy7 labeled anti mouse TCR-β (Clone;H57-597, Biolegend) and APC-Cy7 labeled anti mouse CD11b (Clone;M1/70, Biolegend). Ovalbumin was labeled with Alexa488 2,3,5,6 TFP ester (Invitrogen, Carlsbad, CA) as per the manufacturer's instructions. Unlabeled dye was separated using a 30K cut off membrane specified Amicon Ultra4 centrifugal filter (Millipore, Bedford, MA). Briefly, collagenase digested lymph nodes from immunized mice were counted for absolute cell numbers. Cells were first stained with Alexa430 succinimidyl ester for dead cell staining in PBS for 30 minutes at 4°C. Cells were washed 2× with FACS buffer (PBS with 5% FBS) and stained with PE labeled anti mouse total IgG for 30 minutes at 4°C. Cells were washed 2× and labeled with the all the above mentioned anti mouse surface proteins. Qdot655 labeled streptavidin was used to label the biotinylated anti mouse GL-7 antibodies for another 30 minutes at 4°c. Stained cell samples were fixed with BD Cytofix (BD Biosciences) and acquired on a LSR-II cytometer (BD Biosciences). FACS data was analyzed on Flow JO software. For B cell sorting assays, cells were fluorescently labeled as described above and sorted on a FACS Aria cell sorter (BD Biosciences).

Affymetrix Gene Chip Analysis

Total RNA from sorted B-cells (1.8×10^4 to 1.2×10^6 cells) was purified using Trizol® (Invitrogen, Life Technologies Corporation). All RNA samples were checked for purity using a ND-1000 spectrophotometer (NanoDrop Technologies) and for integrity by electrophoresis on a 2100 BioAnalyzer (Agilent Technologies). The samples were amplified using the Nugen WT Pico Kit (NuGEN Technology) and the target reactions were run with 50ng of Total RNA. The amplification products were processed through the EXON Module (NuGEN Technology) which creates sense-strand cDNA targets. The sense strand cDNA Targets were then fragmented and labeled using NuGEN's FL-Ovation™ cDNA Biotin Module V2 (NuGEN Technology). Labeled targets were hybridized to GeneChip® Mouse Gene 1.0ST arrays (Affymetrix, Inc.), following Standard Nugen Protocols for target hybridization to the Affymetrix Gene Arrays. The hybridizations were run for 16 hours, 45°C, 60RPM in an Affymetrix Hybridization Oven 640. The Cartridge arrays were washed and stained using the Affyemtrix Fluidics Stations 450, following Affymetrix protocols. Scanning was performed on an Affymetrix GeneChip 3000 7G scanner, and Affymetrix GCOS software was used to perform image analysis and generate raw intensity data. Two

independent sets of samples at day 7 post-treatment were used in our analyses. Each set is comprised by B-cells from mice treated with MPL+R837 or from those treated with either individual MPL or R837 alone. Probe sets of all 6 samples were normalized by RMA, which includes global background adjustment and quantile normalization. Each set of samples was subsequently normalized by z-score (number of standard deviation from mean) and treated as biological replicates. Affymetrix chip annotation of GeneChip® Mouse Gene 1.0ST platform was used to annotate and select probe sets that target a known gene (defined as having an Entrez gene ID). Different probe sets that target the same gene were collapsed by taking the probe set with the highest median expression value across all samples. Student's t-test ($p < 0.05$) was used to identify genes differentially expressed in mice receiving MPL +R837 treatment compared to those receiving individual MPL or R837 treatment. A meta-analysis was performed using publicly available microarray data of distinct B cell subsets (plasma, germinal center and memory B cells). Purification strategy, RNA processing method, and hybridization strategy can be found in the original publication 23. Raw microarray data (CEL files of samples GSM94747, GSM94762, GSM94763, GSM94764, GSM94765, GSM94766, GSM94767, GSM94768, GSM94769, GSM94771, GSM94772) were downloaded from NCBI GEO website (GSE4142), and processed by RMA normalization. Affymetrix chip annotation of GeneChip® Mouse Genome 430 2.0 platform was used to annotate and select probe sets that target a known gene (defined as having an Entrez gene ID). Different probe sets that target the same gene were collapsed by taking the probe set with the highest median expression value across all samples. Student's t-test ($p < 0.05$) was used to identify differentially expressed genes (DEGs) between any given 2 B cell subsets. Genes were classified as "plasma DEGs" if they were up-regulated in plasma compared to germinal center and also up-regulated in plasma compared to memory. A similar approach was used to identify "germinal center DEGs" and "memory DEGs".

Genes up- or down-regulated in treatment with MPL+R837 compared to single MPL or R837 treatment were cross-referenced to the genes highly expressed in specific B cell subsets. Fold enrichment was calculated using the formula ('common ZX'/'deg Z')/('subset X'/'total'), where 'common ZX' = number of genes up-regulated in treatment Z (combination of MPL+R837 or individual MPL or R837) and also highly expressed in B cell subset X; 'deg Z' = number of all genes up-regulated in treatment Z; 'subset X' = number of all genes highly expressed in B cell subset X and 'total' = number of all genes in the chip common to both platforms.

H1N1 virus stock preparation

Madin-Darby canine kidney (MDCK) cells (ATCC CCL 34, American Type Culture Collection) were maintained in Dulbecco's modified essential medium (Mediatech Inc., Herndon, VA) containing 10% fetal bovine serum. Stocks of influenza virus strains were prepared by inoculation with H1N1 swine-origin A/California/04/09 strain in allantoic fluid, in 10- or 11-day old embryonated hen's eggs. Virus stocks were harvested from the allantoic fluid. The purity of the virus was determined by SDS polyacrylamide gel electrophoresis in combination with Coomassie blue stain and electron microscopy. The hemagglutination (HA) activity was determined using chicken RBC 0.5% w/v in phosphate buffered saline (PBS) pH 7.2 as previously described 36. The purified virus was inactivated with

formaldehyde at a final concentration of 0.01% (vol/vol), incubated for 72 hrs at 4°C, and then dialyzed against PBS buffer. Inactivation of virus was confirmed by inoculation of the virus into 10-day-old embryonated hen's eggs and plaque assay in MDCK cells 37. We generated mouse adapted A/California/04/09 virus by five serial passages in Balb/c mice. We then determined the LD_{50} for this virus using the Reed-Muench formula 38. For the challenge and infection studies the mice were anesthetized with isoflurane and then infected with virus by intranasal instillation.

H1N1 hemagglutinin inhibition (HAI) assays

Determined as described previously 34.

H5N1 and H1N1 lethal challenge infections

Female Balb/C immunized with the indicated vaccine schedule were anesthetized by intraperitoneal injection of ketamine/xylazine and then intransally infected with 1,000 LD50 of recombinant A/Vietnam/1203/2004 within the enhanced BSL3 Emerging Pathogens Facility at Mount Sinai School of Medicine. To determine survival rates post challenge with mouse adapted A/California/04/09 H1N1 virus, 5 female Balb/C mice per treatment group were challenged 8 weeks post - immunization by intranasal instillation of 30 μl of - 20xLD_{50} - live virus after anesthesia with Isoflurane and monitored for morbidity and mortality upto 14 days. - Animals were humanely euthanized and reported as dead if body weight loss achieved 25%. All H5N1 animal procedures were performed in accordance with guidelines established by the Mount Sinai School of Medicine Institutional Animal Care and Use Committee (IACUC) and National Institutes of Health for the care and use of laboratory animals.

H1N1 -neutralization assays with primate plasma

Sera from non-human primates immunized with swine-origin H1N1 2009 were serially diluted and mixed with 100 pfu of MDCK grown homologous virus for 1 h at room temperature. The mixture was further added to a MDCK cell monolayer and incubated for 45 min at room temperature. The inoculum was removed, wells were overlaid with DMEM agar and incubated for 2 days at 37°C in a 5% CO2 humidified incubator. Then, plates were fixed with 0.25% gluteraldeyde and stained with 1% crystal violet in 20% ethanol, and plaques were counted. Neutralizing antibodies titers were determined as the reciprocal of the serum dilution that decreased by 50% the number of plaques formed by the live virus.

Supplementary Material

Refer to Web version on PubMed Central for supplementary material.

Acknowledgements

We thank Rafi Ahmed and Barry Rouse for discussion and comments on the manuscript. We thank Herold Oluoch for assistance with cryostat sectioning. The work in the laboratory of BP was supported by grants U54AI057157, R37AI48638, R01DK057665, U19AI057266, HHSN266200700006C, NO1 AI50025, U19AI090023, from the National Institutes of Health and a grant from the Bill & Melinda Gates Foundation. Work in AG-S laboratories was partly funded by grants HHSN266200700010C, U54AI57158) and U01AI070469 from the National Institutes of Health.

References

1. Pulendran B, Ahmed R. Translating innate immunity into immunological memory: implications for vaccine development. Cell. 2006; 124:849–863. [PubMed: 16497593]
2. Kawai T, Akira S. The role of pattern-recognition receptors in innate immunity: update on Toll-like receptors. Nat Immunol. 11:373–384. [PubMed: 20404851]
3. Pulendran B. Learning immunology from the yellow fever vaccine: innate immunity to systems vaccinology. Nat Rev Immunol. 2009
4. Querec T, et al. Yellow fever vaccine YF-17D activates multiple dendritic cell subsets via TLR2, 7, 8, and 9 to stimulate polyvalent immunity. J Exp Med. 2006; 203:413–424. [PubMed: 16461338]
5. Querec TD, et al. Systems biology approach predicts immunogenicity of the yellow fever vaccine in humans. Nat Immunol. 2009; 10:116–125. [PubMed: 19029902]
6. Napolitani G, Rinaldi A, Bertoni F, Sallusto F, Lanzavecchia A. Selected Toll-like receptor agonist combinations synergistically trigger a T helper type 1-polarizing program in dendritic cells. Nat Immunol. 2005; 6:769–776. [PubMed: 15995707]
7. Peek LJ, Middaugh CR, Berkland C. Nanotechnology in vaccine delivery. Adv Drug Deliv Rev. 2008; 60:915–928. [PubMed: 18325628]
8. Kazzaz J, et al. Encapsulation of the immune potentiators MPL and RC529 in PLG microparticles enhances their potency. J Control Release. 2006; 110:566–573. [PubMed: 16360956]
9. Singh M, Chakrapani A, O'Hagan D. Nanoparticles and microparticles as vaccine-delivery systems. Expert Rev Vaccines. 2007; 6:797–808. [PubMed: 17931159]
10. Young JA, Collier JR. Attacking anthrax. Sci Am. 2002; 286:48–50. 54-49. [PubMed: 11857900]
11. Chen GL, Subbarao K. Live attenuated vaccines for pandemic influenza. Curr Top Microbiol Immunol. 2009; 333:109–132. [PubMed: 19768402]
12. Hangartner L, Zinkernagel RM, Hengartner H. Antiviral antibody responses: the two extremes of a wide spectrum. Nat Rev Immunol. 2006; 6:231–243. [PubMed: 16498452]
13. Jung S, et al. In vivo depletion of CD11c(+) dendritic cells abrogates priming of CD8(+) T cells by exogenous cell-associated antigens. Immunity. 2002; 17:211–220. [PubMed: 12196292]
14. Kissenpfennig A, et al. Dynamics and function of Langerhans cells in vivo: dermal dendritic cells colonize lymph node areas distinct from slower migrating Langerhans cells. Immunity. 2005; 22:643–654. [PubMed: 15894281]
15. Mata-Haro V, et al. The vaccine adjuvant monophosphoryl lipid A as a TRIF-biased agonist of TLR4. Science. 2007; 316:1628–1632. [PubMed: 17569868]
16. Bernasconi NL, Traggiai E, Lanzavecchia A. Maintenance of serological memory by polyclonal activation of human memory B cells. Science. 2002; 298:2199–2202. [PubMed: 12481138]
17. Pasare C, Medzhitov R. Control of B-cell responses by Toll-like receptors. Nature. 2005; 438:364–368. [PubMed: 16292312]
18. Mitchison NA. T-cell-B-cell cooperation. Nat Rev Immunol. 2004; 4:308–312. [PubMed: 15057789]
19. van Essen D, Dullforce P, Brocker T, Gray D. Cellular interactions involved in Th cell memory. J Immunol. 2000; 165:3640–3646. [PubMed: 11034367]
20. McHeyzer-Williams LJ, McHeyzer-Williams MG. Antigen-specific memory B cell development. Annu Rev Immunol. 2005; 23:487–513. [PubMed: 15771579]
21. Slifka MK, Antia R, Whitmire JK, Ahmed R. Humoral immunity due to long-lived plasma cells. Immunity. 1998; 8:363–372. [PubMed: 9529153]
22. McHeyzer-Williams MG, McLean MJ, Lalor PA, Nossal GJ. Antigen-driven B cell differentiation in vivo. J Exp Med. 1993; 178:295–307. [PubMed: 8315385]
23. Luckey CJ, et al. Memory T and memory B cells share a transcriptional program of self-renewal with long-term hematopoietic stem cells. Proc Natl Acad Sci U S A. 2006; 103:3304–3309. [PubMed: 16492737]
24. Wille-Reece U, et al. HIV Gag protein conjugated to a Toll-like receptor 7/8 agonist improves the magnitude and quality of Th1 and CD8+ T cell responses in nonhuman primates. Proc Natl Acad Sci U S A. 2005; 102:15190–15194. [PubMed: 16219698]

25. Steel J, et al. Live attenuated influenza viruses containing NS1 truncations as vaccine candidates against H5N1 highly pathogenic avian influenza. J Virol. 2009; 83:1742–1753. [PubMed: 19073731]
26. Jurk M, et al. Human TLR7 or TLR8 independently confer responsiveness to the antiviral compound R-848. Nat Immunol. 2002; 3:499. [PubMed: 12032557]
27. Dorner M, et al. Plasma cell toll-like receptor (TLR) expression differs from that of B cells, and plasma cell TLR triggering enhances immunoglobulin production. Immunology. 2009; 128:573–579. [PubMed: 19950420]
28. Clark TW, et al. Trial of 2009 influenza A (H1N1) monovalent MF59-adjuvanted vaccine. N Engl J Med. 2009; 361:2424–2435. [PubMed: 19745215]
29. Potter CW, Oxford JS. Determinants of immunity to influenza infection in man. Br Med Bull. 1979; 35:69–75. [PubMed: 367490]
30. Bachmann MF, Odermatt B, Hengartner H, Zinkernagel RM. Induction of long-lived germinal centers associated with persisting antigen after viral infection. J Exp Med. 1996; 183:2259–2269. [PubMed: 8642335]
31. Sah H. A new strategy to determine the actual protein content of poly(lactide-co-glycolide) microspheres. J Pharm Sci. 1997; 86:1315–1318. [PubMed: 9383747]
32. Henri S, et al. CD207+ CD103+ dermal dendritic cells cross-present keratinocyte-derived antigens irrespective of the presence of Langerhans cells. J Exp Med. 207:189–206. [PubMed: 20038600]
33. den Haan JM, Kraal G, Bevan MJ. Cutting edge: Lipopolysaccharide induces IL-10-producing regulatory CD4+ T cells that suppress the CD8+ T cell response. J Immunol. 2007; 178:5429–5433. [PubMed: 17442923]
34. Zhu Q, et al. Immunization by vaccine-coated microneedle arrays protects against lethal influenza virus challenge. Proc Natl Acad Sci U S A. 2009; 106:7968–7973. [PubMed: 19416832]
35. Staats HF, et al. In vitro and in vivo characterization of anthrax anti-protective antigen and anti-lethal factor monoclonal antibodies after passive transfer in a mouse lethal toxin challenge model to define correlates of immunity. Infect Immun. 2007; 75:5443–5452. [PubMed: 17709410]
36. Compans RW. Hemagglutination-inhibition: rapid assay for neuraminic acid-containing viruses. J Virol. 1974; 14:1307–1309. [PubMed: 4372400]
37. Enioutina EY, Visic D, Daynes RA. The induction of systemic and mucosal immune responses to antigen-adjuvant compositions administered into the skin: alterations in the migratory properties of dendritic cells appears to be important for stimulating mucosal immunity. Vaccine. 2000; 18:2753–2767. [PubMed: 10781863]
38. Reed LJaM H. A simple method of estimating fifty percent endpoints. The American Journal of Hygiene. 1938; 27:493–497.
39. Badr G, et al. Type I interferon (IFN-alpha/beta) rescues B-lymphocytes from apoptosis via PI3Kdelta/Akt, Rho-A, NFkappaB and Bcl-2/Bcl(XL). Cell Immunol. 263:31–40. [PubMed: 20231019]
40. Bekeredjian-Ding IB, et al. Plasmacytoid dendritic cells control TLR7 sensitivity of naive B cells via type I IFN. J Immunol. 2005; 174:4043–4050. [PubMed: 15778362]
41. Thibault DL, et al. IRF9 and STAT1 are required for IgG autoantibody production and B cell expression of TLR7 in mice. J Clin Invest. 2008; 118:1417–1426. [PubMed: 18340381]
42. Tovey MG, Lallemand C, Thyphronitis G. Adjuvant activity of type I interferons. Biol Chem. 2008; 389:541–545. [PubMed: 18953720]
43. Swanson CL, et al. Type I IFN enhances follicular B cell contribution to the T cell-independent antibody response. J Exp Med. 207:1485–1500. [PubMed: 20566717]
44. Liu H, et al. Functional studies of BCL11A: characterization of the conserved BCL11A-XL splice variant and its interaction with BCL6 in nuclear paraspeckles of germinal center B cells. Mol Cancer. 2006; 5:18. [PubMed: 16704730]
45. Smith KG, et al. bcl-2 transgene expression inhibits apoptosis in the germinal center and reveals differences in the selection of memory B cells and bone marrow antibody-forming cells. J Exp Med. 2000; 191:475–484. [PubMed: 10662793]
46. Aiba Y, et al. Preferential localization of IgG memory B cells adjacent to contracted germinal centers. Proc Natl Acad Sci U S A. 107:12192–12197. [PubMed: 20547847]

47. Zhou G, Ono SJ. Induction of BCL-6 gene expression by interferon-gamma and identification of an IRE in exon I. Exp Mol Pathol. 2005; 78:25–35. [PubMed: 15596057]

48. Mitsdoerffer M, et al. Proinflammatory T helper type 17 cells are effective B-cell helpers. Proc Natl Acad Sci U S A. 107:14292–14297. [PubMed: 20660725]

49. Chin AI, et al. TANK potentiates tumor necrosis factor receptor-associated factor-mediated c-Jun N-terminal kinase/stress-activated protein kinase activation through the germinal center kinase pathway. Mol Cell Biol. 1999; 19:6665–6672. [PubMed: 10490605]

50. Basso K, Dalla-Favera R. BCL6: master regulator of the germinal center reaction and key oncogene in B cell lymphomagenesis. Adv Immunol. 105:193–210. [PubMed: 20510734]

51. Kano G, et al. Ikaros dominant negative isoform (Ik6) induces IL-3-independent survival of murine pro-B lymphocytes by activating JAK-STAT and up-regulating Bcl-xl levels. Leuk Lymphoma. 2008; 49:965–973. [PubMed: 18464116]

52. Ke N, Godzik A, Reed JC. Bcl-B, a novel Bcl-2 family member that differentially binds and regulates Bax and Bak. J Biol Chem. 2001; 276:12481–12484. [PubMed: 11278245]

53. Airoldi I, et al. Expression and function of IL-12 and IL-18 receptors on human tonsillar B cells. J Immunol. 2000; 165:6880–6888. [PubMed: 11120812]

54. Airoldi I, et al. Heterogeneous expression of interleukin-18 and its receptor in B-cell lymphoproliferative disorders deriving from naive, germinal center, and memory B lymphocytes. Clin Cancer Res. 2004; 10:144–154. [PubMed: 14734463]

55. Hikida M, et al. PLC-gamma2 is essential for formation and maintenance of memory B cells. J Exp Med. 2009; 206:681–689. [PubMed: 19273623]

56. Nera KP, Lassila O. Pax5--a critical inhibitor of plasma cell fate. Scand J Immunol. 2006; 64:190–199. [PubMed: 16918686]

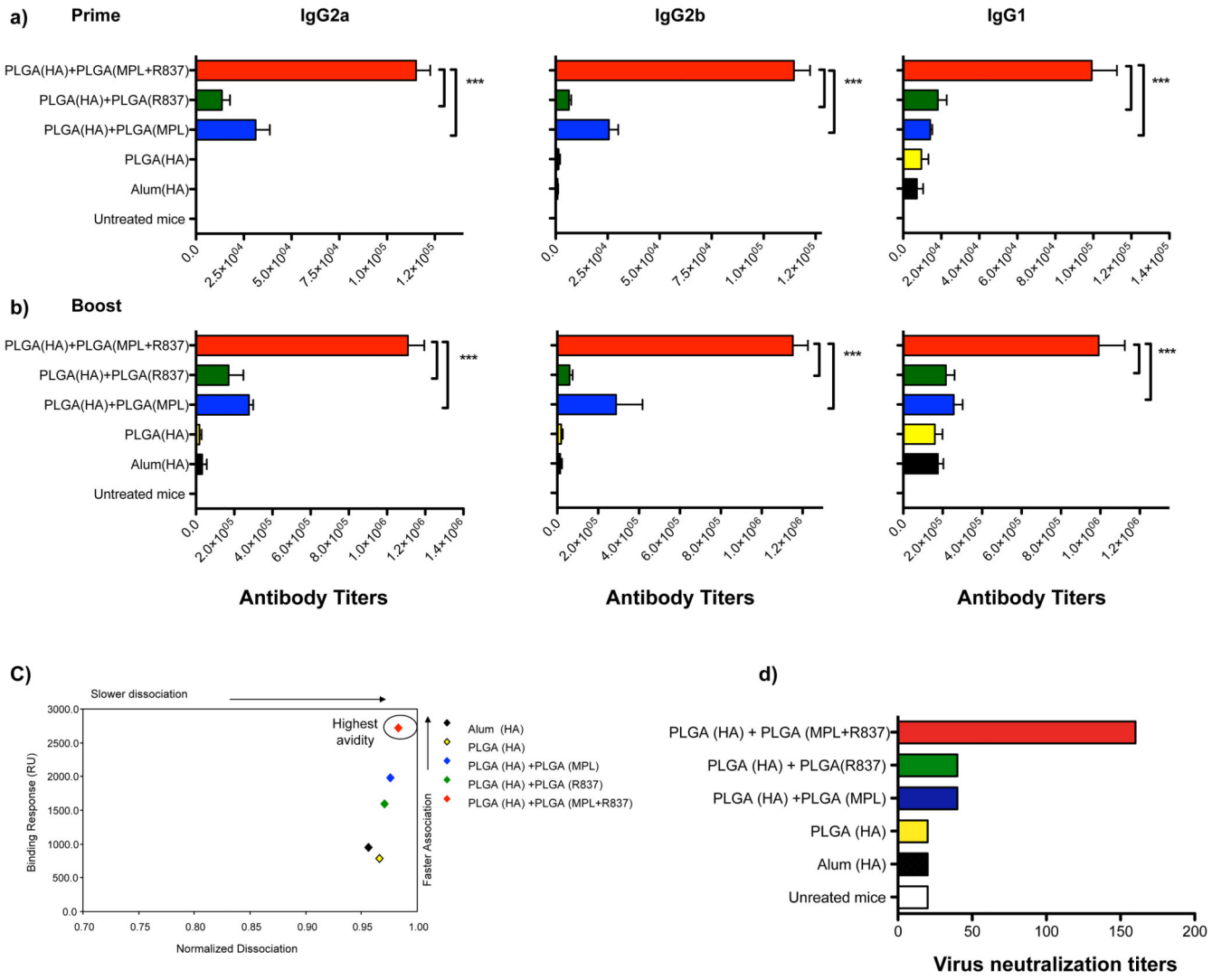

Figure 1. Combination of MPL+R837 in PLGA nanoparticles mediate synergistic enhancement of antibody responses against H5N1 influenza derived HA

a), b) Antibody titers at 4 weeks post primary and secondary immunization (mean + s.e.m of 4 independent experiments, with 4–5 mice /treatment group in each experiment) are shown for IgG2a, IgG2b and IgG1 isotypes. *** represents $p<0.001$ and **$p<0.01$ (one way ANOVA with Bonferroni post hoc test). **c)** Pooled serum samples from HA immunized mice at D28 boost immunization were tested for their HA binding avidity using BIACORE surface plasmon resonance (SPR) based protein binding assay. Data is representative of plots from one of 2 independent experiments. **d)** Virus neutralization assay were performed with pooled serum samples from treatment groups assayed in duplicates. Results shown are representative titers from one of 2 independent experiments.

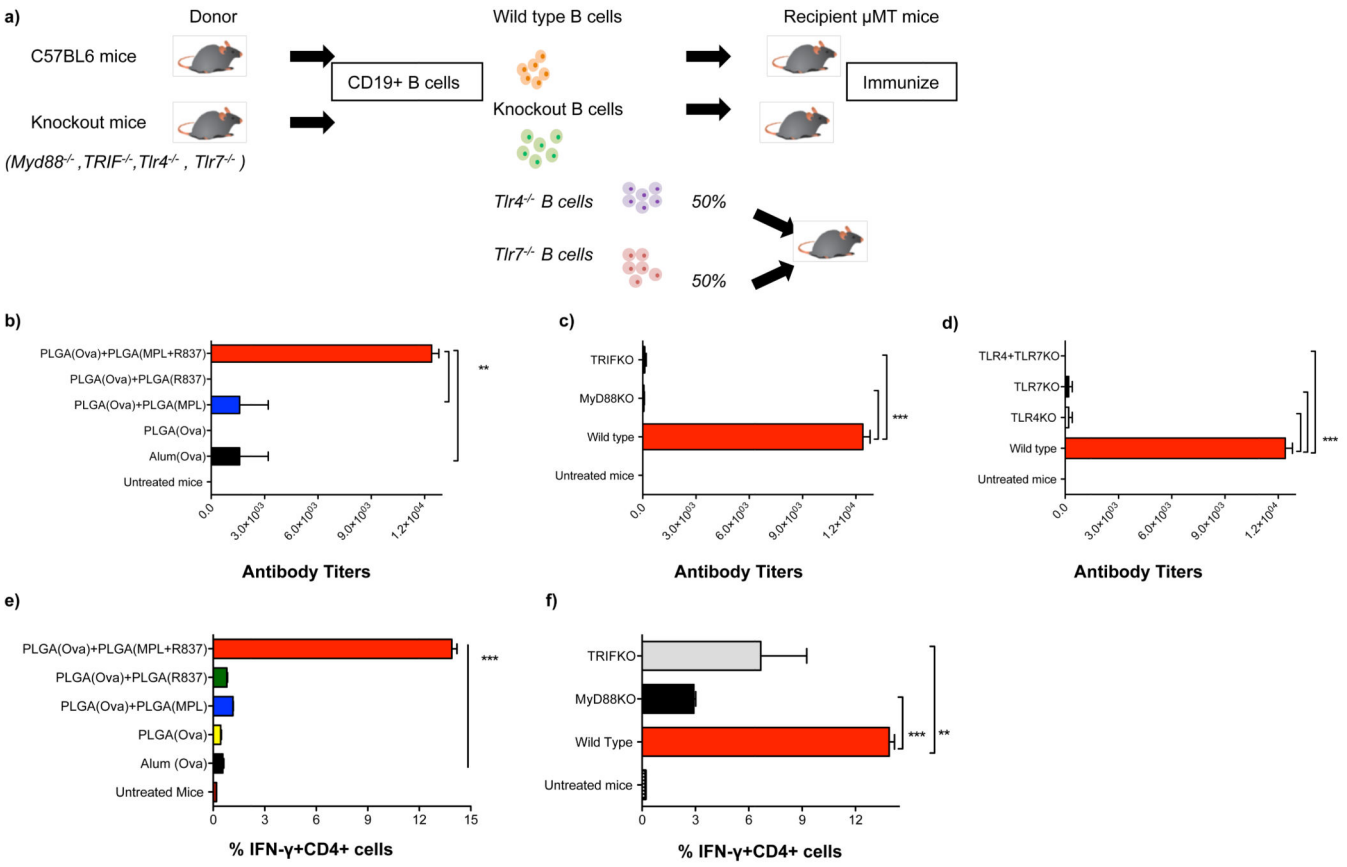

Figure 2. Synergistic enhancement of antibody responses is dependent on the presence of TLRs on B cells

a) B cell deficient mice (μMT mice) were reconstituted with 40 × 10^6 B cells from C57BL/6 mice or from *MyD88*$^{-/-}$, *TRIF*$^{-/-}$, *TLR4*$^{-/-}$ *or TLR7*$^{-/-}$ mice, or equal numbers of *TLR4*$^{-/-}$ and *TLR7*$^{-/-}$ deficient cells to determine whether expression of TLRs and co-expression of TLR4 and TLR7 on the same B cell was necessary for enhancement of antibody responses. Mice were immunized with 10μg of OVA encapsulated in PLGA nanoparticles and adjuvants. **b),c),d)** Mice were bled at D28 post primary immunization and OVA-specific total IgG antibody responses were determined using ELISA. Antibody titers are shown (mean + s.e.m of 2 independent experiments, with 3 mice /treatment group in each experiment). *** represents $p<0.001$ and **$p<0.01$ (one way ANOVA with Bonferroni post hoc test). **e)** The magnitude of OVA-specific IFN-γ producing memory CD4+ T cells in the draining lymph nodes of μMT mice is shown with representative FACS plots. **f)** The magnitude of OVA-specific IFN-γ producing memory CD4+ T cells in the draining lymph nodes is dependent on MyD88 and TRIF expression on B cells. Graphs represent mean frequencies ± s.d of triplicate cultures of pooled lymph node cells from one out of 2 independent experiments.

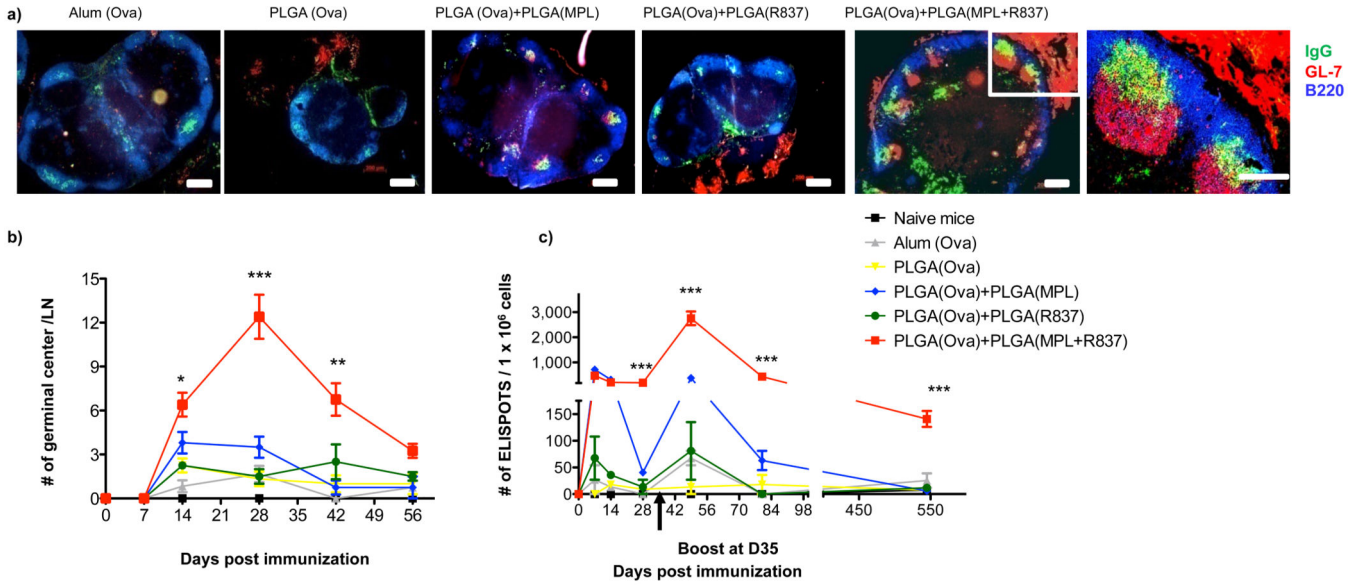

Figure 3. Immunization with nanoparticles containing MPL+R837 induces persistent GCs and long lived antibody forming cells in draining lymph nodes

a) C57BL/6 mice were immunized with OVA encapsulated in nanoparticles with MPL +R837 plus antigen. 4 weeks post primary immunization draining lymph nodes were excised, tissue sections prepared and stained for GCs (GL-7 red, B220 blue and IgG green). Images are representative of 2 independent experiments with draining lymph nodes obtained from at 2–3 mice per treatment condition per experiment. **b)** GCs were counted in LN sections at the time points indicated and represented as mean ± s.e.m from 4–6 draining lymph nodes from n=2–3 mice/treatment group. **c)** ELISPOT assay. Combination of TLR4 and TLR7 ligands has no effect on the short lived ASCs, but stimulates long lived ASCs that persist for ~1.5 years. Graph represents average spots per 1×10^6 total lymph node cells ± s.e.m from duplicate cultures per treatment group. Data is representative of at least 2–3 independent experiments per time point indicated.

a)

Group	# of Rhesus Macaques	Antigen, (WIV)	Adjuvant
1	4	10μg	
2	4	10μg	PLGA(MPL+R837)
3	4	10μg	PLGA(MPL+R848)
4	4	50μg	

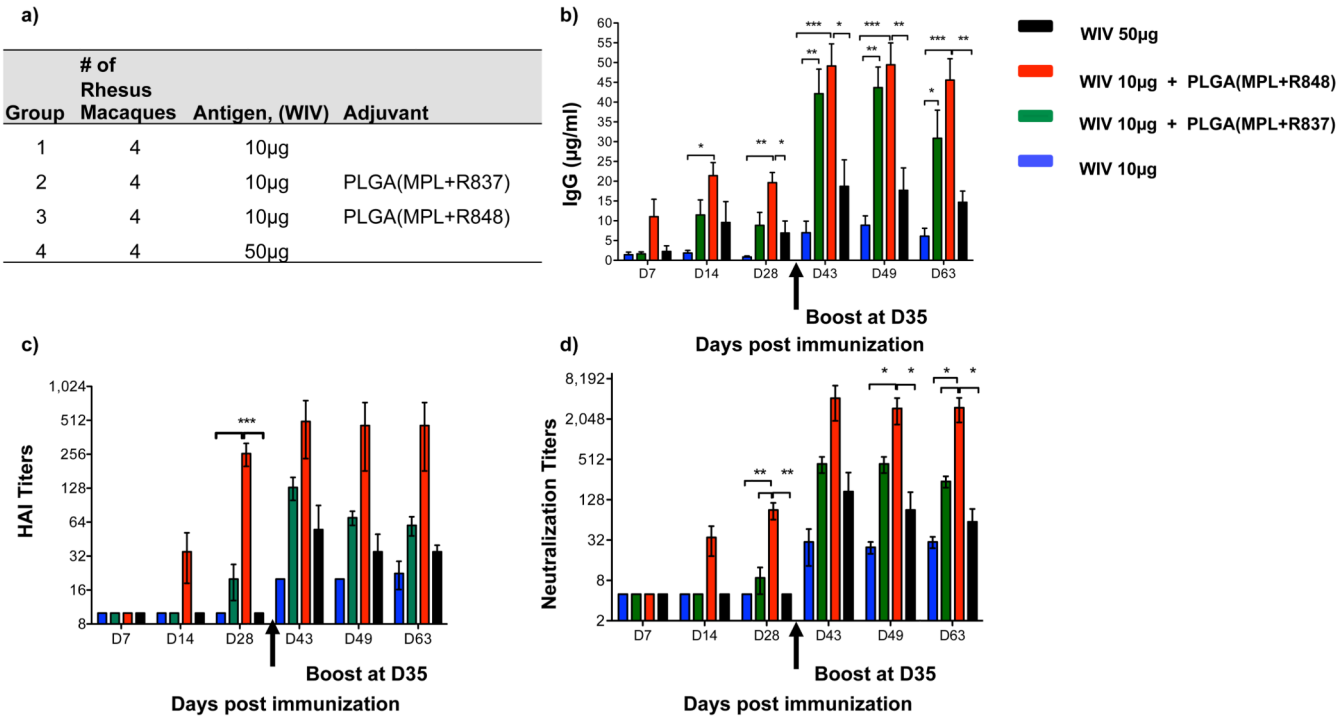

Figure 4. Immunization of Rhesus macaques with 2009 pandemic H1N1 influenza A, whole inactivated virus (WIV), plus nanoparticles containing MPL+R837 or MPL+R848 induces robust humoral immune responses

a) Rhesus macaques (n=4) were immunized with 10μg of H1N1 WIV with or without nanoparticle encapsulated MPL+R837 or MPL+R848. 50μg of MPL and 750μg of R837 and R848 encapsulated in nanoparticles was used per animal. One group of 4 animals was also immunized with 50μg of WIV to determine dose sparing effects mediated by adjuvants. **b)** Antibodies against WIV were analyzed as described in the materials and methods and results are represented as mean ± s.e.m. **c)** HAI titers were assayed at indicated time points and are represented as mean ± s.e.m. **d)** Neutralization titers as represented as the reciprocal of the plasma dilution that decreased the number of plaques formed by the live virus by 50%. Statistical significance was analyzed by ANOVA (Bonferroni post hoc test) and indicated on the figures wherever significant. *** represents $p<0.001$, **$p<0.01$ and *$p<0.05$.